Original Article

Institution of MECHANICAL ENGINEERS

Journal of ENGINEERING FOR THE MARITIME ENVIRONMENT

Proc IMechE Part M:
J Engineering for the Maritime Environment
2024, Vol. 238(2) 262–272

DOI: 10.1177/14750902231213449
journals.sagepub.com/home/pim
Sage

Investigation of oil emission mechanisms in a marine medium-speed dual-fuel engine

Baptiste Hochfellner[1], Friedrich Wirz[1], Konstantin Pryymak[2], Ann-Christin Preuß[2] and Gerhard Matz[2]

Abstract

Pilot-ignition Otto marine engines are known for greatly reduced emissions of air pollutants (sulphur oxides, nitrogen oxide, particulates) compared to marine diesel engines. However, lubricating oil emissions still are about one order of magnitude higher than in land-based systems. To identify reduction potentials, a better understanding of oil emission mechanisms has to be gained. For this purpose, mass spectrometric oil emission measurements and fluorescence lubricating film thickness measurements were performed on a medium-speed marine engine. With the fluorescence measuring system, the varying lubricating oil film on the cylinder wall can be visualised and analysed in sub-crank-angle resolution. By applying the developed calibration method to the measurement data, the oil film thickness can be determined in μm. It is shown that the oil film left by the piston rings on the liner as it moves down is almost halved after ignition compared to during intake stroke. The authors have further been able to detect and time operating point dependent ring rotation and investigations show a connection between ring rotation and cylinder liner temperature distribution. Aligning ring gaps allow blow-by to happen. This and other high intensity events such as engine knock, load shedding or the transition from diesel-mode to gas-mode, heavily disturb the oil layer and cause peaking oil emissions.

Keywords

Marine engineering, oil emissions, oil film, large bore engines, dual-fuel engines, LNG, fluorescence method

Date received: 14 July 2023; accepted: 23 October 2023

Introduction

Combustion engines have been one of the leading drivers for global economic growth since the early 20th century. Especially in the shipping industry, diesel engines are being used due to their great reliability, durability, wide range of power, very high efficiency and comparably safe operation. Light motor vehicles benefit from Otto engines which have a higher power-to-weight ratio and generally are smaller. Due to the principle of combustion – an ideally homogeneous air-fuel mixture is compressed and ignited via an external source, for example a spark plug – Otto engines produce less harmful emissions than diesel engines. Generation of nitrogen oxides is less likely due to lower peak temperatures. Generation of parti culates is much lower due to the cleaner combustion of the near-homogeneous mixture. Sulphur oxides cannot be generated because common Otto fuels do not contain sulphur.[1]

While harmful pollution has been a concern for a long time and thus have led to the implementation of strict (mostly national) regulations and policies for emissions from power plants and motor vehicles, emissions from international shipping have not been regulated until the adoption of MARPOL Annex VI in 2005. Today, global regulations regarding air pollution from ship engines exist for nitrogen oxide emissions and maximal allowed sulphur content in fuels. Additionally, IMO has adopted a number of so-called emission control areas (ECA), where stricter limits are applied. Limits to particulate emissions have not yet been applied.[2]

[1]Department of Marine Engineering (ASM), Hamburg University of Technology, Hamburg, Germany
[2]Institute for Analytical Measurement Technology Hamburg eV (IAM), Hamburg, Germany

Corresponding author:
B Hochfellner, Department of Marine Engineering (ASM), Hamburg University of Technology, Am Schwarzenberg-Campus 4(c), Hamburg 21073, Germany.
Email: b.hochfellner@tuhh.de

One important stepping stone on the path to a cleaner future of shipping has been the use of liquefied natural gas (LNG) as fuel. This led to the introduction of a new engine type into the maritime world, that is neither an Otto nor a diesel engine. In gas operation, this engine type uses LNG as main fuel which is mixed with the charge air, compressed as a mixture and then ignited. These are characteristics of an Otto engine. However, the ignition of the mixture comes from the autoignition of a pilot fuel that is injected into the compressed mixture. This is the main characteristics of a diesel engine. Accordingly, this engine type comes with some of the advantages and disadvantages of both worlds. Since diesel fuel has to be present on board anyway, these engines are usually designed to be able to perform full range in diesel operation as well. This requirement and the unique conditions of life at sea have contributed to the fact, that marine engines consume about one order of magnitude more lubricating oil per kWh than stationary gas-engines. This consumption is almost exclusively happening in the piston-liner-group and the consumed lubricating oil leaves the engine via the funnel and thus contributes to oil emissions, see Adolf et al.,[2] Woodyard.[3]

Although it is unlikely that LNG will be the dominating fuel of the future, many of the so-called future fuels are Otto fuels that will need a pilot diesel fuel for ignition in medium-speed marine engines. The Department of Marine Engineering (ASM) at Hamburg University of Technology, Germany, has equipped their dual-fuel engine test bench with extensive oil measurement systems developed and operated by Institute for Analytical Measurement Technology Hamburg e.V. (IAM), Germany. The presented work has been carried out with a medium-speed engine because these engines are increasingly used where humans are living and working in the vicinity and thus air quality plays a particularly important role. This includes usage as main propulsion of ships that are frequently operating near coasts and in waterways, such as cruise liners, ferries and smaller cargo ships. Furthermore, in large cargo ships these engines serve as auxiliary power units to generate electricity during port layovers.

This paper highlights oil film and exhaust gas measurements and how the results pave the way to reduced oil emissions.

Oil emissions

The reduction of oil emissions has been of scientific interest in the automotive sector for decades. In Germany the research association FVV eV has contributed a lot to the current state of knowledge, by funding and accompanying many research projects including FVV-nos. 1124,[4] 1197[5] and 1302[6] from the Piston Ring Oil transport cluster as well as FVV-nos. 1084[7] and 1225[8] from the Fuel in Oil cluster. Oil emissions have been linked to the lube oil film thickness, for example, the amount of oil present, and lube oil consumption. Different oil transport mechanisms have been identified and categorised into their effect on oil emissions. Reverse-blow-by has been found to be a major mechanism of oil transport towards the combustion chamber and as such of oil emissions. Generally speaking, the results show the necessity to co-develop piston rings and cylinder liners in a way that the rings are able to seal the combustion chamber under all relevant operation conditions with low lube oil consumption. This was described by the above as well as Hadler et al. [9] There is a wide number of measures that can be combined to achieve these goals: From the cylinder liner's perspective the honing was developed further a lot. Modern honing techniques from plateau honing to spiral glide honing to contour honing have found their way into the market.[10] Newer publications, such as by Hellwig,[11] Böhm[12] and Hrdina et al. [13] describe benefits of varying honing properties over the length of the cylinder liner (e.g. stratum honing).

Most of the research is concerning spark-ignited otto engines from the automotive sector.

Recently, more and more research is being published for heavy-duty on- and off-road diesel engines. Since particulate emissions in diesel engines are dominated by unburnt fuel emissions (e.g. soot), research is more focussed on fuel-oil interaction and lube oil consumption rather than oil emissions, as seen in Zhang et al.,[14] Pasligh et al.[15] Due to the mechanisms being related, findings also show the above-mentioned necessity to co-develop piston rings and cylinder liners.

There is little published research on medium-speed four-stroke dual-fuel engines, regarding the above topics, as deployment of this engine type is a relatively new development in a secluded market with particularly long service lives and few engine component manufacturers.

Engine test bench

The single-cylinder engine test bench was originally put into operation in 1998 representing a typical medium-speed marine engine with the capability to burn the wide range of diesel fuels that is being used in shipping.[3] It is based on a common base frame with a directly coupled water vortex brake and an intermediate bearing. Basis for its design by AVL List is the MAN 32/40 series – named after its characteristic values of a bore of 32 cm and a stroke of 40 cm – and most of its parts are MAN components of this series. Being a research engine, it has been equipped with abundant measurement technology and comes with some extraordinary features, such as independently controlled charge air pressure and exhaust back pressure, thus simulating the capability of different turbochargers, and full electronic control over various parameters regarding the engine as well as its simulated environment.

Over the years the test bench has received many upgrades, such as a modern PLC control, a common-rail system and updated measurement systems. Within the latest major retrofit an additional natural gas fuel system was added. It is now a so-called dual-fuel engine with the possibility for full range diesel operation as well as full range pilot-ignited gas operation. The main fuel in gas operation is either liquefied natural gas (LNG) which is stored in an insulated type-C pressure tank at approximately −160°C or any other compliant fuel compressed to up to 300 bar, stored in gas cylinders. To ensure valid test results for maritime applications, the whole system is in compliance with national landside as well as international maritime regulations, for example, IGF code (IGF Code - International Code of Safety for Ships Using Gases or Other Low-Flashpoint Fuels - Part A – 2.2.28 (https://www.imorules.com/GUID-8F1C7A20-E399-4D7F-BB38-0A09DF149FF7.html)). As of the date this paper is submitted, an upgrade to the capability to burn liquid future fuels (e.g. methanol) is in the planning phase.

The main characteristics of the current engine layout are listed in Table 1, operational parameters for gas operation are listed in Table 2.

This dual-fuel engine type is one important step that is being implemented by the industry for the transition from traditional diesel operation to a fully sustainable future. It has the benefit of fuel choice depending on the circumstances, regarding regulations, availability and costs. When in gas operation, emission of particulates and nitrogen oxides is greatly reduced due to its Otto engine characteristics. This engine type can easily comply to IMO TIER III without exhaust gas aftertreatment. Since natural gas does not contain sulphur, any existing regulation regarding sulphur in shipping is also met. However, this engine type also comes with some drawbacks. The compromises that have to be made in order for it to be operated in two very different operational modes make it impossible for it to reach the full potential of either a diesel engine or a fully optimised gas engine with regard to efficiency, emissions and power range. Also, many shipowners hesitate to use liquefied natural gas due to safety concerns, investment costs and operational challenges. On top of that, although fossil natural gas contains less carbon than Diesel fuels and its use in shipping is beneficial regarding EEDI, EEXI and CII ratings (The EEDI (Energy Efficiency Design Index), EEXI (Energy Efficiency Existing Ship Index) and CII (Carbon Intensity Indicator) are mandatory energy efficiency standards set by IMO within their greenhouse gas strategy 16), it does not on its own save enough on carbon dioxide emissions to be suitable for the reduction goals from the Paris agreement of 2015 that have been adopted by International Maritime Organization[16] within its greenhouse gas strategy. That being said, these engines are still very important to pave the way to the desired future. Synthetic methane, a fully renewable fuel when derived from green electricity, can be used in these engines.[2] Also, a lot of what can be learned from operating this engine type as a research engine, can be transferred to engines, that use liquid future fuels, as long as combustion is initiated by pilot ignition of (possibly synthetic) diesel fuel.[1]

Table 1. Main engine parameters.

Parameter	Value
Engine type	Medium-speed four-stroke dual-fuel, single cylinder
Gas mode	Port fuel injection, Pilot fuel ignition
Primary fuel	LNG/CNG
Pilot / secondary fuel	Diesel, via common rail at 1600 bar
Bore	320 mm
Stroke	400 mm
Stroke-to-bore ratio	1.25
Compression ratio	12
Piston ring layout	2× compression ring 1× oil scraper ring
Lubrication system	Dry sump lubrication
Cylinder lubrication	Oil supply via ducts in liner
Charging	Variable (compressor unit)
Exhaust back pressure	Variable (adjustable valves)

Table 2. Nominal operational parameters of the engine in gas operation.

Nominal parameters (gas operation)	Unit	Value
Engine speed	rpm	750
Mean piston speed	m/s	10
Power	kW	372
Break mean effective pressure	bar	18.5
Torque	kNm	4.7
Charge air pressure	bara	4.2

Approach

To investigate the lubricating oil mechanisms in the tribology system consisting of piston, piston rings and cylinder liner with its effects on emissions, a combination of optical oil film thickness and oil emission measurements was used on the medium-speed marine engine (Figure 1). Although the measurement application of the engine is very extensive overall, this paper focuses on the application of the fluorescence measurement technique for oil film thickness measurement and the correlation of the observed phenomena with oil emission, quantified by mass spectrometry.

Fluorescence measurement system

The previously developed measurement system, based on the principle of fluorescence, has been adjusted to enable measurements on the cylinder liner of a marine engine, see Hochfellner et al.[17] This system (Figure 2) consists of LEDs as light source, photodetectors for

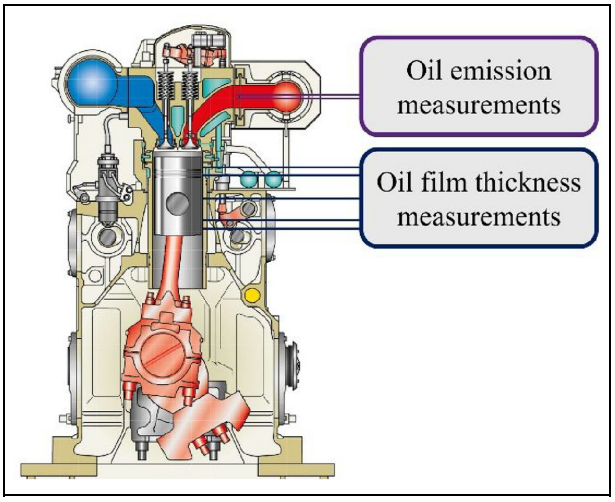

Figure 1. Engine cross section with measurement systems.

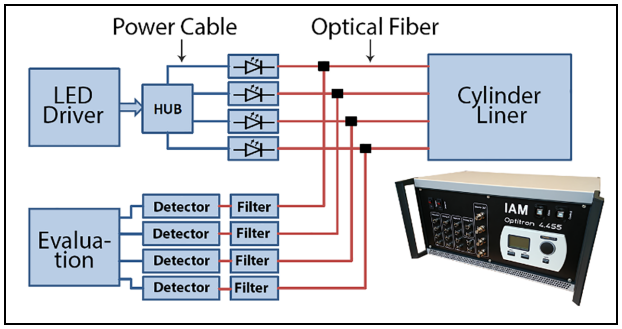

Figure 2. Fluorescence measuring system with diagram.

recording of fluorescence radiation and step-index multimode optical fibres for data transmission. LEDs were used as the excitation source for the fluorescence, which significantly reduces the technical measurement effort. If a fluorescent substance is present at the measuring point directly in front of the optical fibre end (e.g. the oil film on the liner), it is excited and the resulting emitted radiation, together with the possibly reflected LED radiation, is directed to the detectors. The optical filters mounted directly in front of the detectors allow only the wavelengths of the fluorescent light to pass through. Due to the proportional relationship of the detector signal to the radiation intensity and thus also to the quantity of the substance at the measuring point, film thickness of the substance in front of the measuring point can be determined by evaluating the data using the calibration signals. Liquids that have no or very low intrinsic fluorescence can be mixed with a fluorescent agent.

A main limitation of the fluorescence measuring principle as described above is the dependence of the fluorescence on the temperature. Consequently, when applying this principle to the engine, on the one hand the temperature of the oil must be known, which is

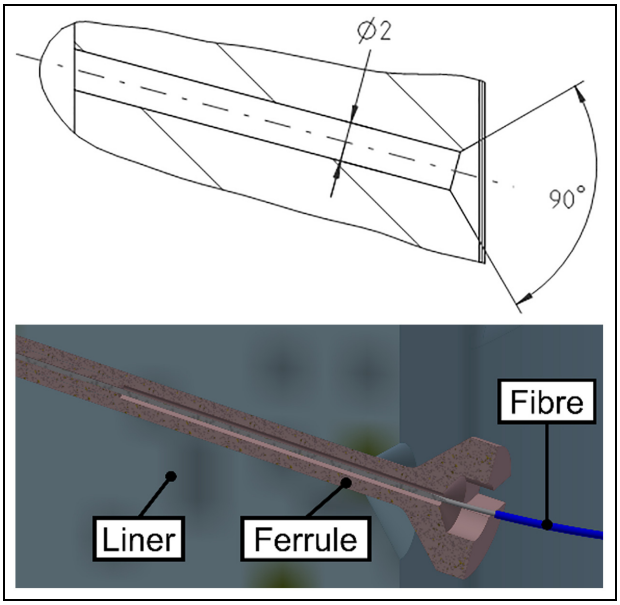

Figure 3. Fluorescence measurement point design. Top: Through holes in cylinder wall. Bottom: Ferrule inside cylinder wall with optical fibre (cutaway view).

measured via thermocouples near the measuring points, and on the other hand the temperature must also be considered during calibration.

The calibration of the data measured according to this principle is involved with additional difficulties. In addition to the required temperature-calibration-parameter, other influencing variables must be taken into account, such as the measurement position-, wear-, oil quality-, sensor line- and channel-calibration parameters. Calibration devices for the relation of the detector signal and radiation intensity are part of the measuring system.

This measurement system was successfully applied to the MAN 32/40 dual-fuel engine (ASM). The application included mainly two parts:

- fitting the new cylinder liner with measuring positions/sensors
- providing the lubricating oil with fluorescent properties

Measuring positions. The measurements are conducted via optical fibres, that puncture the cylinder wall at different angles and positions. To ensure the specifications of the application, which are

- minimal liner/engine geometry adaptation,
- structural strength of the cylinder liner,
- fibres interchangeability/repairability,

the optical fibres are glued into so-called ferrules which in turn are glued into the Ø 2 mm drill holes of cylinder liner. These ferrules are constructed as shown in Figure 3 and made of a material with similar mechanical and

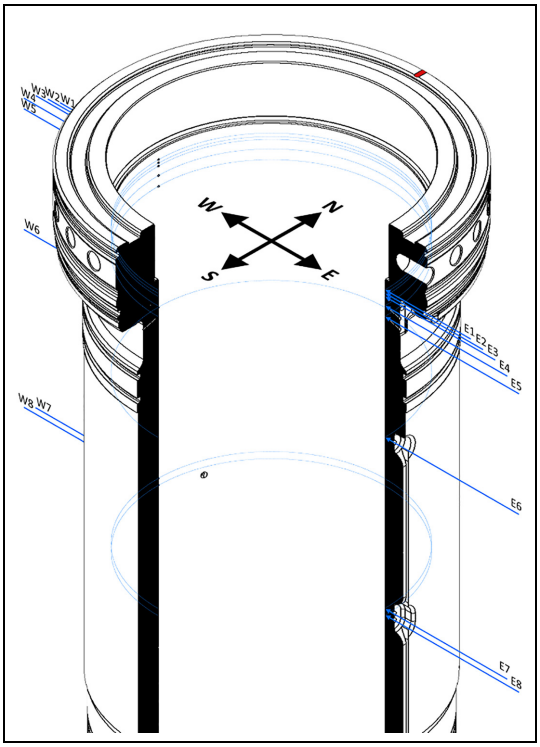

Figure 4. The new cylinder liner with positions of the optical fibres. The top five, the sixth and the bottom two layers correspond to the top-dead-centre (TDC), high-piston-velocity and bottom-dead-centre (BDC) section, respectively. North (N) is pointed towards the output shaft.

thermal properties as the cylinder liner itself. The measuring surface of the ferrules as well as the optical fibres glued into them is concave polished. Optical fibres are installed perpendicular to the cylinder surface or at an approximately 75° angle to avoid the collision with the sealing ring.

The structural integrity of the cylinder liner with its adaptions was calculated in FEM analysis. Calculated deformations due to temperatures, clamping forces and gas forces are similar to the untreated liner.

To reduce the total number of measurement positions they are placed only on the exhaust gas side and air supply side, where the piston lateral forces are most abundant. Following the spacial definition shown in Figure 4, these are the east (E) and the west (W) positions, respectively. In this figure north (N) is pointed towards the output shaft. As for the vertical positions, three main sections have been determined. Top-dead-centre (TDC) and bottom-dead-centre (BDC) positions as well as a high piston-velocity section in between the former two. The total number of optical fibres installed into the cylinder liner is 16.

Fluorescence of lubricating oil. The lubricating oil of the engine has low intrinsic fluorescence. For successful measurements a fluorescent agent has been added to the lubricating oil. This substance has to meet the required fluorescent properties while not changing the

Figure 5. Lubrication oil after mixing with the fluorescent agent.

properties of the oil or be harmful to the engine test bench in any way. The agent shall stay in solution at all times and not agglomerate, deposit or build foam during engine operation and long periods of downtime without heating. For this reason, flocculating tests and mass spectrometric examination of mixed lubrication oil were carried out successfully. Lumilux CD 345 manufactured by Honeywell International Inc. was used as the fluorescent agent within this project. It has proved its worth in other research projects due to its good fluorescence properties, see Uhlig et al.,[5] Stein et al.[18] This powdery substance is mixed with the engine oil in a constant ratio (between 0.10 and 0.12% m.m) to obtain a fluorescent solution (Figure 5). Reduced mixing ratio of 0.05% was chosen for first engine measurements to investigate the segregation or filter clogging and was further increased to 0.10%. During the course of the project, the fluorescent agent mostly stayed in solution, only after multiple weeks of downtime sedimentation could be found at the bottom of the oil tanks. After running the oil cycle at temperature for a few hours the mixture got back to its former fully dissolved state. Filtres did not clog.

Oil emission measurement system

Mass spectrometric oil emission measurement is widely used in research and development in the field of passenger car engines. Due to the high temporal resolution of this method, not only steady-state but also transient engine operation can be investigated, see Hadler et al.,[9] Mahle,[19] Frommer et al.[20]

The oil emission is quantified using the high-pass filter method described by Gohl,[21] which does not require the use of a tracer substance in the oil. The unburned hydrocarbons in the exhaust gas of internal combustion engines originate from both the fuel and the lubricating oil. However, molecular masses of hydrocarbons in the fuel are lower. According to this standard method for quantifying the total oil emission of internal combustion engines a high-pass filter can be defined to summary quantify the oil-borne hydrocarbons. As diesel

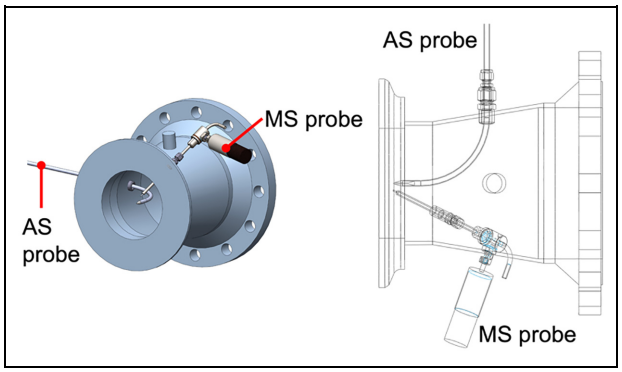

Figure 6. Positioning of sampling probes in the exhaust pipe.

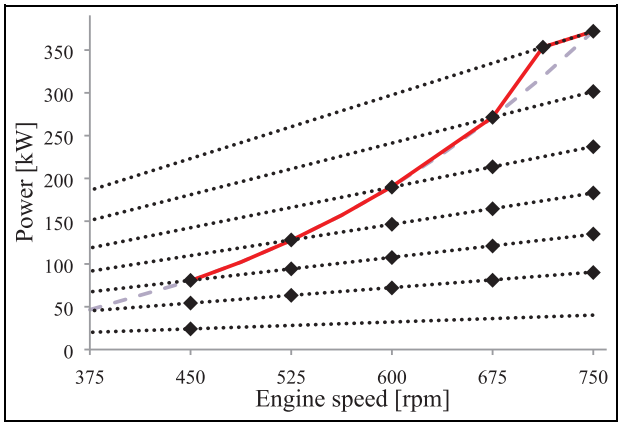

Figure 7. Engine map with operating points.

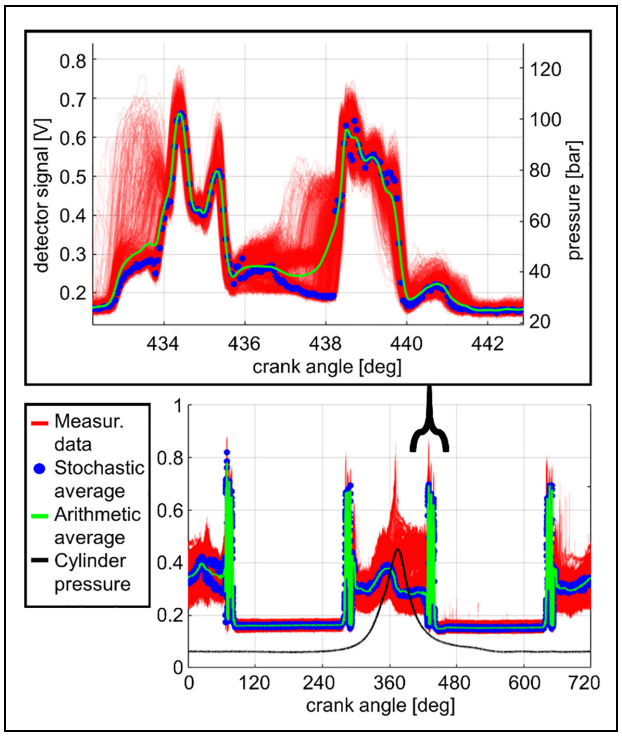

Figure 8. Oil film thickness measurement. Top: Data between 433 and 443°ca when passed by piston rings. Operation point: 525 RPM, 1.72 kNm, 1626 cycles, Measurement point: W6 (high velocity).

fuel is used for pilot ignition, a filter limit of m/z 270 was applied here. Calibration is performed using an oil vapour gas sample with a defined concentration.

The oil emission measurement system used is the LUB360 from the company Lubrisense. It is based on a QTOF (quadrupole-time-of-flight) mass spectrometer and is equipped with a heated direct inlet system to prevent condensation of exhaust gas sample components.

In addition, an aerosol spectrometer (Welas 2070H by Palas), based on the principle of light scattering, was applied to the engine to quantify the aerosol particle emission, which includes thrown off oil droplets. A sampling system that conditions an exhaust gas sample to the specifications of this sensor was developed in a previous research project for passenger car engines, see Gohl et al.[22] This system was modified to allow the aerosol spectrometer to be used in the entire engine map of this medium-speed marine engine.

Figure 6 shows the set-up of the measuring probes for both systems in the exhaust pipe. The probes for mass spectrometry (MS) and aerosol spectrometry (AS) are applied in the same plane as close as possible to the exhaust valve for uniform sampling.

Measurement results

To generate the measurement results, engine maps and individual operating points with respect to the engine's operating limits were carried out. The engine map of the test bench is shown in Figure 7. Power delivery is limited at the top by its maximum defined load for the current engine settings (red line). A characteristic curve with a correlation of Power to Speed $P \sim n^3$ is displayed as well (dashed grey curve). This curve corresponds to a typical operational curve of a ship with a fixed pitch propeller. All marked operating points are located on a dotted line of equal torque. However, not all of these have been investigated during the course of this project due to cost savings.

During engine runs in 2020 and 2021 the above described measurement systems have been successfully deployed and performed nominally. In this section, selected observed phenomena are discussed.

Cylinder liner oil measurements

The oil film thickness measurements described in this section are presented partly as calibrated and partly as uncalibrated data. Due to the difficulties of calibration, the oil film thickness cannot be presented as data over time or crank angle, but can be divided into sections and calculated over several working cycles. Moreover, there is a clear difference between the arithmetic and stochastic average of the signals (stochastic averages = mode of probability mass function).

An example measurement is shown in Figure 8. The red data shows the oil film thickness of over 1600 working cycles. In this example the passing of the first and second piston rings can be seen. The film thickness

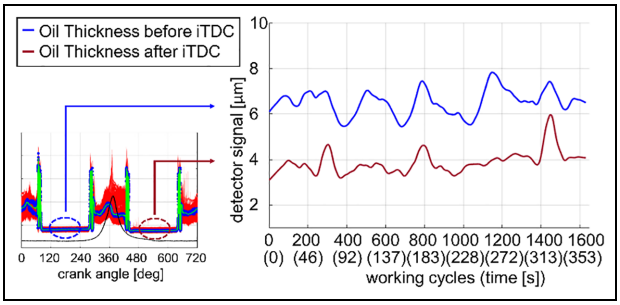

Figure 9. Oil film thickness measurement. Right: Averaged data in micrometres before and after iTDC. Operation point: 525 RPM, 1.72 kNm, 1626 cycles, Measurement point: W6 (high velocity).

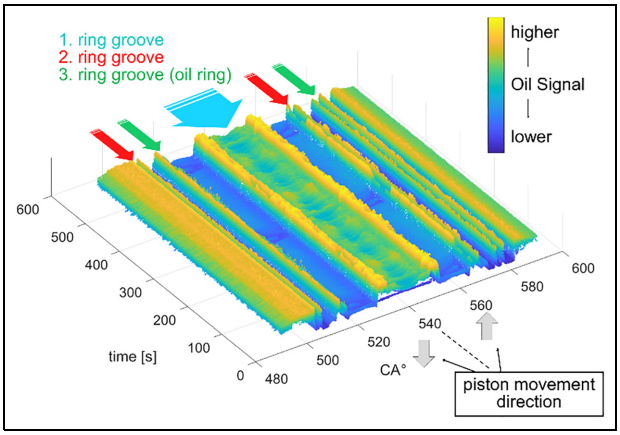

Figure 10. Oil film thickness measurement. Passing of the piston ring pack in the BDC. Operation point: 750 RPM, 1.72 kNm, 3065 cycles, Measurement point: W8 (BDC).

must not be directly concluded from the height of the values at the piston-rings-times compared with the piston-skirt-times, since the calibration factors are quite different.

Using this measurement as an example, the following characteristic features can be seen. The film thicknesses during the passage of the piston geometries (piston rings, piston ring pack shoulders, piston skirt shoulders) are subject to higher fluctuations or scattering and therefore the consideration of different mean values is meaningful. Furthermore, an oil collar can be detected that is pushed directly in front of the piston rings. Here it is recognisable before 434°ca (degree crank angle) and 438°ca with higher fluctuations in the signal. In addition, the surface shape of the passing parts can be well recognised in the measurement data (crowning of ring 2 is higher).

When evaluating this data, it is divided into sections of the constant conditions in front of the measuring point. In the example of the measurement in Figure 8, the measuring point is located in the high piston-velocity section and is passed by the piston with its three piston rings followed by a time period without the piston in front of it.

The time periods of the measurement data that are the simplest to evaluate in terms of oil film thickness, are the sections when the piston is not in front of the measuring point and the combustion flames are already gone. In Figure 9 two sections of the above mentioned 1600 cycles are grouped and shown over the motor runtime. In the section between 120°ca and 240°ca the piston is below the measuring point *before* iTDC (ignition top-dead-centre) and in the section between 480°ca and 600°ca the piston is below the measuring point *after* iTDC. Taking into account the calibration parameters (oil factor, temperature factor, light guide factor), film thicknesses in micrometres can be calculated from this. These data are shown in the figure on the right, where the film thickness before iTDC is, as expected, higher than after iTDC due to higher gas pressure during combustion. The averaged oil thickness data shown here before and after combustion is subject to periodic fluctuation.

An important aspect of the measurement results is the wear of the measuring points in the upper area (TDC section). These measuring positions are exposed to significantly higher temperatures and pressures. Furthermore, they are influenced by the combustion flame.

To illustrate the behaviour of the lubrication oil on the liner, it is useful to extend the representation of the data to the time axis. For a better understanding of the data, a measurement at the measuring position in the BDC section on the intake side (W) is described below. Essentially, the type of displayed data in Figure 10 is the same as in Figure 8, except that individual work cycles are displayed over time, so that a map of the oil behaviour is apparent. In this diagram a section of data is shown between 480°ca and 600°ca while the piston passes BDC. Furthermore, the sections are marked while the piston rings pass the measuring position. Note that the speed of the piston decreases as it approaches BDC (540°ca), which is reflected in the width of the individual ring sections. As previously explained, the oil signal on the crankshaft axis (CA°) cannot be directly compared with each other because individual sections require their own calibration factors. Nevertheless, individual areas such as the rings/ring-lands can be compared with each other respectively as well as the progressions of the signals over time (time axis). Numerous aspects of oil behaviour can be identified in this way. Figure 11 is an enlarged representation of the measurements from Figure 10 where the individual rings can be better identified as the piston moves upward (after 540°ca). The oil collar can be seen under the first compression ring as it moves down and stops at the measuring position and then moves up again (530°ca & 550°ca). Such oil collar is also visible on the second ring below and above the ring as it moves upward (565°ca). However, the oil collar can only be seen below the second ring as it moves downwards before BDC (515°ca).

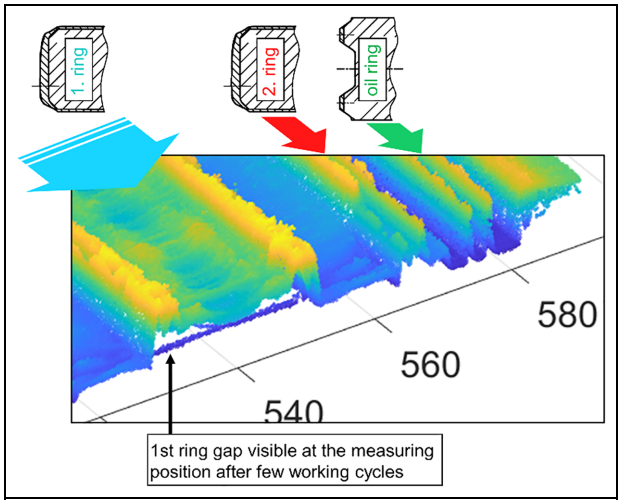

Figure 11. Oil film thickness measurement. Detailed view after the BDC. Operation point: 750 RPM, 1.72 kNm, 3065 cycles, Measurement point: W8 (BDC).

Another aspect of the oil behaviour can be observed in Figure 11, which is due to the ring gap of the first ring. This ring gap is visible a few seconds after the start of the measurement in the first ring section. In addition, the influences of the ring gap on the area between the first and second rings and on the oil on the second ring are visible.

For a better understanding of the ring gaps and the rotation of the rings, the data can be displayed during the passing of the piston, on both sides of the liner (East & West) for a longer period of time. This data is shown in Figure 12, as a top-view representation at measuring positions in BDC section. Here, the areas during the occurrence of the first ring gap at the measuring point are marked. From these data can be concluded that the first ring has a continuous rotation at this operating point, since the ring gap can be seen alternately on the east and west sides of the liner. A detailed examination of the data reveals no significant rotation of the second piston ring and the oil scraper ring. The behaviour of the oil as well as the piston rings changes depending on the motor speed/load combinations.

The influence of the piston ring rotation on the liner temperature and the oil emission in the exhaust gas obtained from these data are described in the following section. Further phenomena can be observed when examining other operating points. Among them are for example, the rotation of the oil scraper ring or depletion of the lubricating layer during the transition of the engine operation type.

Oil emission caused by ring rotation

The fluorescence measurement technique has shown its usefulness in researching of lubricating oil behaviour in the tribology system as well as ring rotation observation. An essential step in this research is the analysis of the oil emission mechanisms under the inclusion of all available engine and measurement data. In the following, the observed correlation of the ring rotation and the oil emission in the exhaust gas is described.

In certain operating conditions, especially during low load, significant variations of oil emission in the exhaust gas could be detected. Considering the simultaneously acquired measurement data, especially the cylinder liner temperatures as well as the oil layer on the liner, a clear correlation was identified.

Figure 13 shows all essential data for this observation. The data at the top of the graph shows the fluctuating

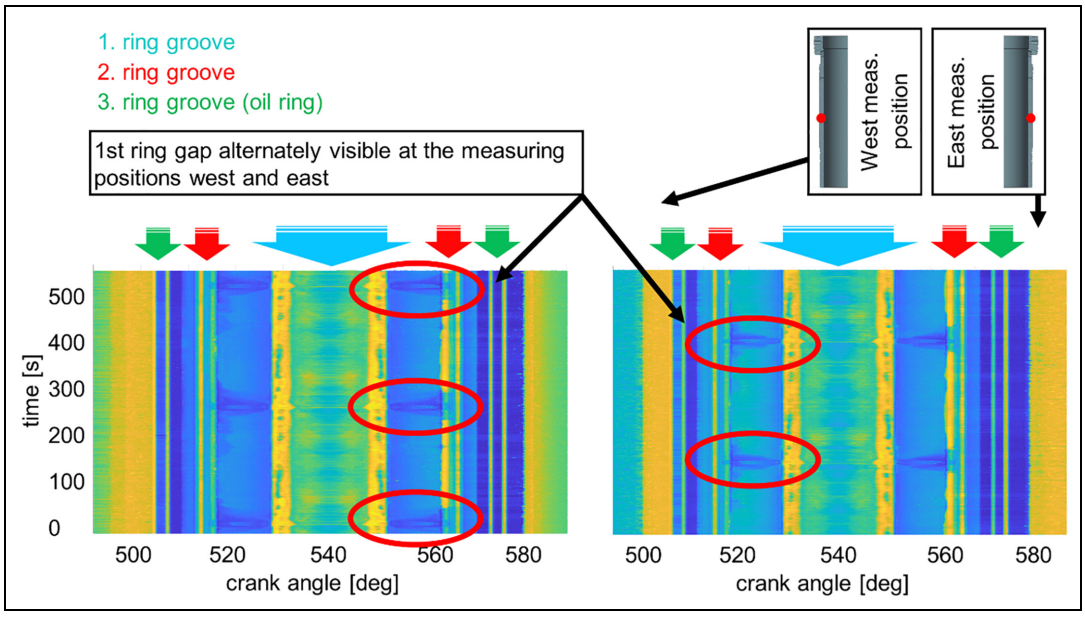

Figure 12. Oil film thickness measurement. Detecting the first ring gap. Operation point: 750 RPM, 1.72 kNm, 3065 cycles, Measurement points: W8 & E8 (BDC).

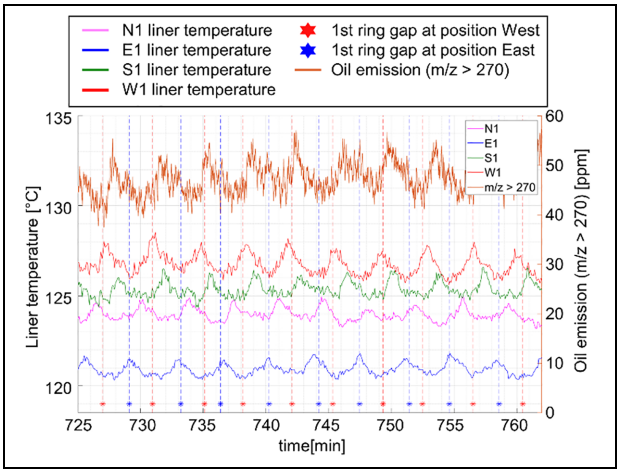

Figure 13. Combined measurement results during first ring gap rotation. Operation point: 750 RPM, 1.72 kNm.

oil emission in the exhaust gas. The four coloured profiles show the temperature data in the upper area of the liner (red, green, pink, blue). And finally dots in the bottom part of the graph show the occurrence of the first ring gap at the measuring points on the east (blue) and west (red) sides of the liner. It can be easily observed that the periods of the respective fluctuations coincide. On the one hand the oil emission is directly influenced by the overlap of the ring gaps of the first and second ring which leads to blow-by (an increased gas flow through the piston ring group). On the other hand it might also be influenced by a possible deformation of the liner caused by liner temperature fluctuations as a consequence of the blow-by. In a further engine run, a cyclic fluctuation of the aerosol particle concentration in the exhaust gas synchronous with the oil emission fluctuations was also observed. Oil droplets, which can be either thrown off by inertia forces in TDC or increased blow-by, are not only detected by the mass spectrometer but also by the aerosol particle measurement system.

Furthermore, the direction of rotation of the first ring as well as the position of the ring gap of the second ring can be approximated from this observation. According to the trend of the four temperature-sensors data the direction of rotation of the first piston ring is counterclockwise. And consequently, the position of the second ring gap has to be in the south region. Investigations of further operating points regarding the operating parameters and extensive measurement results are promising.

Summary and conclusion

In order to achieve the goal of reducing marine engine emissions resulting from the entry of lubricating oil into the combustion chamber, it is necessary to understand the correlations between the oil transport phenomena in the tribological system consisting of piston, piston rings and cylinder liner and the resulting oil emissions. Based on this knowledge, specific emission reduction measures can be developed. In this context, findings from the automotive sector are not directly transferable, since not only the geometric conditions but also the requirements for operational safety and the general operating conditions differ significantly. The successful application of the extensive measurement technology described here for analysing the oil film in the combustion chamber and the oil emission in the exhaust gas of this marine medium-speed dual-fuel engine provides the possibility to specifically look for emission reduction measures for this engine type.

The fluorescence measurement technique already made it possible to visualise interesting phenomena within the tribology system, which at the same time demonstrate the measurement capability of the system with respect to the oil film. The temporal resolution of the system allows sub-crank angle resolved investigation of the oil transported by the piston rings. A periodic oscillation of the mean oil film thickness on the liner over multiple working cycles was observed. By applying the developed calibration method to the measurement data, the oil film thickness can be determined in μm. The analysis shows that the oil film left by the piston rings on the liner as it moves down is almost halved after ignition (high gas pressure) than during intake stroke (low gas pressure).

Furthermore, simultaneous investigations with the fluorescence and oil emission measurement techniques identified the cause of an oil emission phenomenon that leads to significantly increased oil emissions during stationary operation. If the ring gaps of the compression rings overlap during ring rotation, this results in an increased gas flow through the piston ring group (blow-by), which leads to increased oil emission values. In the measurements described here, continuous ring rotation of approximately 1/5 RPM was observed, resulting in cyclically fluctuating oil emission with 25% deviation. High blow-by values must therefore be prevented for low-emission operation.

The knowledge gained about the fundamental relationships between oil transport mechanisms in the tribology system and oil emissions, is used to identify emission-reducing measures. The measurement systems also offer the possibility of verifying these measures and evaluating their efficiency. Continuous measurement of the film thickness on the liner ensures that the friction-reducing effect of the lubricating film is sufficiently maintained by the measures taken because operational safety is a top priority in marine applications.

Further research

Following the promising results of the combination of the measurement systems it is planned to use them with varying cylinder liner and piston/piston ring layouts in a follow-up project that is currently being worked out by the research team and industry partners. Since blow-

by effects have been identified to disturb the oil film thoroughly and lead to increased oil emission, it is planned to redesign piston rings and liner surface in such a way that blow-by is minimised and lube oil emission is reduced. Piston ring variations in differently honed liners are to be investigated. The measurement systems allow to precisely observe the influences of individual components.

As mentioned in the introduction, an upgrade to the engine that would enable it to process liquid future fuels (e.g. methanol) is in the planning phase. The combination of measurement systems as presented in this paper is also part of the plans for further research projects with liquid future fuels.

With regard to optimising the measurement systems, the positioning and the application of the cylinder liner oil measurements will be extended by additional measurement points in a horizontal plane. This will increase the radial resolution of the ring gap tracking. Honing of the cylinder liner with preinstalled optical fibres rather than installing optical fibres after honing may further improve signal strength.

In the development of further emission reduction measures, simulation software by AVL is used. The measurement data obtained by engine runs serve as validation variables for the current engine setup. Subsequently, component variations carried out in the simulation and their resulting influence on oil film thickness and oil emissions will provide the basis for further measures that are then to be experimentally validated on the research engine.

Acknowledgement

The authors would like to thank FVV eV, Frankfurt, Germany, for ongoing support and funding of the development of the lubricating oil film thickness measurement system presented in this paper during project no. 1327 'Lubrication Large Bore Engines'.

Declaration of conflicting interests

The author(s) declared no potential conflicts of interest with respect to the research, authorship, and/or publication of this article.

Funding

The author(s) received no financial support for the research, authorship, and/or publication of this article.

ORCID iD

B Hochfellner https://orcid.org/0000-0003-4862-0156

References

1. Merker GP and Teichmann R. *Grundlagen Verbrennungsmotoren: Funktionsweise und Alternative Antriebssysteme Verbrennung, Messtechnik und Simulation*. Wiesbaden: Springer-Verlag, 2019.
2. Adolf J, Balzer C, Kofod M, et al. 2019. Verflüssigtes Erdgas. Neue Energie für Schiff und Lkw? Fakten, Trends und Perspektiven. Shell LNG-Studie.
3. Woodyard D. *Pounder's marine diesel engines and gas turbines*. Oxford: Butterworth-Heinemann, 2009.
4. Kirner C, Uhlig B, Behn A, et al. 2015 Öltransport durch die Kolbenringe, FVV no. 1124: Kolbenring Öltransport I, Frankfurt: Research Association for Combustion Engines eV.
5. Uhlig B, Kirner C, Preuß A-C, et al. 2017. Piston Ring Oil Transport (II). FVV no. 1197. Frankfurt: Research Association for Combustion Engines eV.
6. Schäffer J. *Piston ring oil transport – glassliner 2, FVV no. 1302*. Frankfurt: Research Association for Combustion Engines eV, 2019.
7. Seel K, Geppert A, Meister C, et al. 2016 Fuel in Oil, FVV no. 1084, Frankfurt: Research Association for Combustion Engines eV.
8. Ebert T and Preuß A-C. *Fuel in oil II – sources of oil in combustion chamber of SI engines, FVV no. 1225*. Frankfurt: Research Association for Combustion Engines eV, 2019.
9. Hadler J, Lensch-Franzen C, Gohl M, et al. Concept for analysing and optimising oil emission. *MTZ Worldw* 2014; 75(1): 24–29.
10. Schmid J. Reibungsoptimierung von Zylinderlaufflächen aus Sicht der Fertigungstechnik. *MTZ - Motortechnische Z* 2010; 71(6): 408–413.
11. Hellwig T. 2014 Simulation der Kolbengruppe und deren Interaktion mit der Zylinderlaufbahn. Doctoral dissertation. Technische Universität München
12. Böhm HP. 2018, Neue Anforderungen bringen neue Herausforderungen für Honprozess & -maschine, 5. Győrer Tribologie- und Effizienztagung, Győr.
13. Hrdina D, Maurizi M, Lemm B, et al. Variably honed cylinder liners, iron-based cast pistons and variably coated piston rings as PCU system for friction loss and TCO reduction. In: Siebenpfeiffer W (ed.) *Heavy-Duty, On-und Off-Highway Motoren 2019*. Wiesbaden: Springer Vieweg, 2019, pp.83–98.
14. Zhang J, Zhang G, He Z, et al. Analysis of oil consumption in cylinder of diesel engine for optimization of piston rings. *Chin J Mech Eng* 2013; 26(1): 207–216.
15. Pasligh H, Köser PS, Berbig F, et al. Reibungsminimierung durch Mikrostrukturen auf der Zylinderlaufbahnoberfläche. *MTZ - Motortechnische Z* 2021; 82(5–6): 40–45.
16. IMO. 2023. IMO Strategy on reduction of GHG emissions from ships. Annex 1 Resolution MEPC.377(80)
17. Hochfellner B, Preuß AC, Pryymak K, et al. 2021 Lubrication Large Bore Engines I – Reduction of lube-oil related emissions of particulate matter and hydrocarbins, FVV no. 1327, Frankfurt: Research Association for Combustion Engines eV.
18. Stein C, Budde M, Krause S, et al. 2009. Schmierölemission und Gemischbildung – Beeinflussung der Schmierölemission durch die Gemischbildung im Brennraum von Verbrennungsmotoren. FVV no. 933. Frankfurt: Research Association for Combustion Engines eV

19. Mahle GMBH. *Pistons and engine testing*. Wiesbaden: Vieweg + Teubner Verlag/Springer Fachmedien Wiesbaden GmbH, 2012.
20. Frommer A, Beeckmann A, Freier R, et al. Analysis of Lube Oil Consumption in transient engine operation. *MTZ Worldw* 2013; 74(1): 26–33. 2013.
21. Gohl M. *Massenspektrometrisches Verfahren zur dynamischen Online-Messung der Ölemission von Verbrennungsmotoren*. Düsseldorf: VDI-Verlag, 2004.
22. Gohl M, Matz G, Preuß A-C, et al. 2018. Investigation of oil sources in the combustion chamber of direct injection gasoline engines. SAE Technical Paper, no. 2018-01-1811.